0026-895X/08/7306-1596–1609$20.00
MOLECULAR PHARMACOLOGY
Vol. 73, No. 6
43612/3333856
Mol Pharmacol 73:1596–1609, 2008
Printed in U.S.A.

MOL PHARM

Activation of Corticotropin-Releasing Factor Receptor 1 Selectively Inhibits $Ca_V3.2$ T-Type Calcium Channels[S]

Jin Tao, Michael E. Hildebrand, Ping Liao, Mui Cheng Liang, Gregory Tan, Shengnan Li, Terrance P. Snutch, and Tuck Wah Soong

Department of Physiology, Yong Loo Lin School of Medicine, National University of Singapore, Singapore (J.T., P.L., M.C.L., G.T., T.W.S.); Michael Smith Laboratories, University of British Columbia, Vancouver, Canada (M.E.H., T.P.S.); Department of Pharmacology, Nanjing Medical University, Nanjing, China (J.T., S.L.); and Department of Neuroscience, Johns Hopkins University School of Medicine, Baltimore, Maryland (T.W.S.)

Received November 19, 2007; accepted February 21, 2008

ABSTRACT

The corticotropin-releasing factor (CRF) peptides CRF and urocortins 1 to 3 are crucial regulators of mammalian stress and inflammatory responses, and they are also implicated in disorders such as anxiety, depression, and drug addiction. There is considerable interest in the physiological mechanisms by which CRF receptors mediate their widespread effects, and here we report that the native CRF receptor 1 (CRFR1) endogenous to the human embryonic kidney 293 cells can functionally couple to mammalian $Ca_V3.2$ T-type calcium channels. Activation of CRFR1 by either CRF or urocortin (UCN) 1 reversibly inhibits $Ca_V3.2$ currents (IC_{50} of ~30 nM), but it does not affect $Ca_V3.1$ or $Ca_V3.3$ channels. Blockade of CRFR1 by the antagonist astressin abolished the inhibition of $Ca_V3.2$ channels. The CRFR1-dependent inhibition of $Ca_V3.2$ channels was independent of the activities of phospholipase C, tyrosine kinases, Ca^{2+}/calmodulin-dependent protein kinase II, protein kinase C, and other kinase pathways, but it was dependent upon a cholera toxin-sensitive G protein-mediated mechanism relying upon G protein $\beta\gamma$ subunits ($G\beta\gamma$). The inhibition of $Ca_V3.2$ channels via the activation of CRFR1 was due to a hyperpolarized shift in their steady-state inactivation, and it was reversible upon washout of the agonists. Given that UCN affect multiple aspects of cardiac and neuronal physiology and that $Ca_V3.2$ channels are widespread throughout the cardiovascular and nervous systems, the results point to a novel and functionally relevant CRFR1-$Ca_V3.2$ T-type calcium channel signaling pathway.

The corticotropin-releasing factor (CRF) family, consisting of CRF, urocortin 1 (UCN), UCN2, and UCN3, are critical regulators of stress and inflammatory responses, and they have been variously associated with being cardioprotective and contributing toward alcohol and drug dependencies (Reul and Holsboer, 2002; Bale and Vale, 2004; Bruijnzeel and Gold, 2005; Gravanis and Margioris, 2005). The two major receptors for CRF and UCNs, CRF receptor (CRFR)1 and CRFR2, have been identified as G protein-coupled receptors (GPCRs) that can mediate responses via activation of the protein kinase signaling pathways (Bruijnzeel and Gold, 2005; Gravanis and Margioris, 2005). CRF has a higher affinity for CRFR1 than for CRFR2, UCN shows high affinity for both CRFR1 and CRFR2, whereas UCN2 and UCN3 are selective for CRFR2 (Bale and Vale, 2004). The CRFR1 is expressed primarily in the brain and pituitary, and activation of CRFR1 exerts numerous central and peripheral effects associated with pathological diseases (Dautzenberg and Hauger, 2002). Within the hypothalamus-pituitary axis, CRF and CRF-related peptides such as UCN activate CRFR1 receptors to regulate pituitary function in response to stress

T.W.S. is supported by grants from the Biomedical Research Council, Singapore. T.P.S. is supported by an operating grant from the Canadian Institutes for Health Research and a Canada Research Chair.

Article, publication date, and citation information can be found at http://molpharm.aspetjournals.org.

doi:10.1124/mol.107.043612.

[S] The online version of this article (available at http://molpharm.aspetjournals.org) contains supplemental material.

ABBREVIATIONS: CRF, corticotropin-releasing factor; UCN, urocortin(s); CRFR, corticotropin-releasing factor receptor; GPCR, G protein-coupled receptor; HEK, human embryonic kidney; RGS, regulator of G protein signaling; MAS-GRK3, G protein-coupled receptor kinase; RT-PCR, reverse transcription-polymerase chain reaction; TBST, Tris-buffered saline/Tween 20; I-V, current-voltage; PTX, pertussis toxin; CTX, cholera toxin; GF-109203X, 3-[1-[3-(dimethylaminopropyl]-1*H*-indol-3-yl]-4-(1*H*-indol-3-yl)-1*H*-pyrrole-2,5-dione monohydrochloride; H-89, *N*-[2-(4-bromocinnamylamino)ethyl]-5-isoquinoline; KN-93, 2-(*N*-[2-hydroxyethyl])-*N*-(4-methoxybenzenesulfonyl)amino-*N*-(4-chlorocinnamyl)-*N*-methylamine; U-73122, 1-[6-[[17β-methoxyestra-1,3,5(10)-trien-17-yl]amino]hexyl]-1*H*-pyrrole-2,5-dione; PKA, cAMP-dependent protein kinase; $G\beta\gamma$, G protein $\beta\gamma$ subunit; GDPβS, guanosine-5′-*O*-(2-thiodiphosphate); GTPγS, guanosine-5′-*O*-(3-thiotriphosphate); PLC, phospholipase C; PKC, protein kinase C; TK, tyrosine kinase(s); ET-18-OCH_3, 1-*O*-octadecyl-2-*O*-methyl-rac-glycero-3-phosphocholine; CaMKII, Ca^{2+}/calmodulin-dependent protein kinase II; PI3K, phosphatidylinositol 3-kinase; RT, reverse transcriptase; PKI 5-24, protein kinase A inhibitor fragment 5-24.

(Reul and Holsboer, 2002; Bale and Vale, 2004). In addition, overactive CRFR1 receptors in extrahypothalamic circuits have been implicated in affective disorders (Reul and Holsboer, 2002).

Low-voltage-activated calcium channels play critical roles in thalamocortical processes in both the awake and sleep states, pacemaking activity, action potential burst firing (Steriade and Llinas, 1988), and pain transmission and hormone secretion (Perez-Reyes, 2003; Hildebrand and Snutch, 2006). In mammals, three α_1-subunit genes have been described that encode distinct low voltage-activated calcium channels (T-type) with unique biophysical and pharmacological properties: $Ca_V3.1$ (α_{1G}), $Ca_V3.2$ (α_{1H}), and $Ca_V3.3$ (α_{1I}) (Perez-Reyes, 2003). Previous reports have shown that $Ca_V3.1$, $Ca_V3.2$, and $Ca_V3.3$ are differentially and widely expressed in brain and various peripheral tissues (Cribbs et al., 1998; McKay et al., 2006; Molineux et al., 2006). Altered T-type calcium channel activity has been implicated in cardiac hypertrophy (Nuss and Houser, 1993), generalized epilepsies (Nelson et al., 2006), and both acute and chronic pain signaling (Bourinet et al., 2005). Although the electrophysiological properties of Ca_V3 T-type channels are primarily regulated by dynamic changes in membrane potential, their functional properties can also be modulated by the actions of hormones or neurotransmitters acting via GPCRs that trigger downstream transduction pathways (Welsby et al., 2003; Wolfe et al., 2003; Chemin et al., 2006; Kim et al., 2006).

UCN, an endogenous agonist for CRF receptors, has been shown to either attenuate or stimulate low threshold calcium currents depending on the type of native cells examined (Lee and Tse, 1997; Tao et al., 2005; Kim et al., 2007). Various T-type calcium channel subtypes are expressed in these cells (Jagannathan et al., 2002); however, because of the lack of discriminatory antagonists, the selective inhibitory effect of CRFR1 activation on each of the three Ca_V3 channels—$Ca_V3.1$, $Ca_V3.2$, and $Ca_V3.3$—could not be investigated pharmacologically in these cells. As CRFR1, Ca_V3 and various calcium channels are localized to peripheral and central neuron regions, including the amygdala, hippocampus, hypothalamus, and pituitary (Chalmers et al., 1995; Talley et al., 1999), it is of interest to ask by what mechanism does the activation of the CRFR1 underline the inhibition of Ca_V3 channels and to ask whether the Ca_V3 calcium channels are specifically inhibited.

In the present study, we report that activation of CRFR1 endogenous to the HEK293 cells selectively inhibited $Ca_V3.2$ calcium channels, whereas $Ca_V3.1$ and $Ca_V3.3$ channels were not affected. Besides, the mechanism for the inhibition was mediated via a cholera-toxin sensitive, G$\beta\gamma$-dependent pathway. It is noteworthy that the decrease in $Ca_V3.2$ currents was due to a novel mechanism involving the hyperpolarized shift in the steady-state inactivation property of the channels, and the effect is reversible upon washout of the CRFR1 agonists. As UCN affect multiple aspects of cardiac and neuronal physiology and as $Ca_V3.2$ channels are expressed widely throughout the cardiovascular and nervous systems, our results point to a novel and functionally relevant CRFR1-calcium channel signaling pathway.

Materials and Methods

Cell Culture and Transient Transfection Protocols. HEK293 cells were maintained in Dulbecco's modified Eagle's medium + 10% fetal bovine serum. Transient transfection was performed using the standard calcium phosphate transfection method with a DNA mix containing 1:9 ratios (by weight) of green fluorescent protein plasmid and constructs encoding for rat or human $Ca_V3.1$, $Ca_V3.2$, and $Ca_V3.3$ isoforms. The full-length rat (McRory et al., 2001) and human (kindly provided by David Parker, Neuromed Pharmaceuticals, Inc., Vancouver, BC, Canada) $Ca_V3.1$, $Ca_V3.2$, and $Ca_V3.3$ α_1-subunits were cloned into the pcDNA3 vector (Invitrogen, Carlsbad, CA). RGS2 and MAS-GRK3 constructs (both kindly provided by Dr. Brett Adams, Utah State University, Logan, UT) were subcloned into pEGFP-C2 and pIRES vectors, respectively (Clontech, Mountain View, CA).

Reverse Transcription-Polymerase Chain Reaction. Total RNA was extracted from HEK293 cells using the RNeasy kit (QIAGEN, Valencia, CA). Reverse transcription was carried out with SuperScript II (Invitrogen). Negative control (reactions without reverse transcriptase) was carried out in all RT-PCRs to exclude contamination. The sequences of the primers used in this study are summarized in Supplemental Table 1. Hypothalamus and left cardiac atrium were used as positive controls for the expression of CRFR2α and CRFR2β, respectively. The expression of β-actin mRNA was examined as an internal control. The PCR protocol includes a denaturation step at 95°C for 2 min, and the denaturation, annealing, and elongation cycle was carried out at 94°C for 30 s, at 65°C (CRFR1, R2α, and R2β) or 60°C (β-actin) for 20 s, and at 72°C for 1 min. PCR was carried out for 35 cycles (CRFR1, R2α, and R2β) or 25 cycles (β-actin), respectively. PCR analysis was repeated at least twice with the same samples to confirm reproducibility of the results.

Western Blotting. HEK293 cells were lysed for 1 h in buffer containing 1% Triton X-100, 10 μg/ml aprotinin, and 1 mM phenylmethylsulfonyl fluoride in phosphate-buffered saline (PBS). After centrifugation at 40,000 rpm for 30 min at 4°C, 30 μg of soluble protein was separated in 10% SDS-polyacrylamide gel. The proteins were then transferred electrophoretically onto polyvinylidene difluoride membrane (Bio-Rad Laboratories, Hercules, CA) using a semi-dry transfer system (Bio-Rad Laboratories) with methanol omitted from the transfer buffer. For immunolabeling experiments, membranes were first incubated with 5% nonfat milk in TBST (20 mM Tris, pH 7.6, 137 mM NaCl, and 0.05% Tween 20) for 1 h at room temperature. The membranes were then incubated with diluted primary antibody anti-CRFR1 (1:500 dilution, V-14; Santa Cruz Biotechnology, Inc., Santa Cruz, CA) or anti-CRFR2 (1:500 dilution, C-15; Santa Cruz Biotechnology, Inc.) at 4°C overnight. After five washes with TBST, membranes were incubated for 2 h with 2000-fold diluted rabbit anti-goat secondary antibody (Sigma-Aldrich, St. Louis, MO). After another five washes with TBST, the specific binding of the primary antibody was detected with SuperSignal West Pico chemiluminescent substrate (Pierce Chemical, Rockford, IL). The intensities of immunoreactive staining were measured using a scanning densitometer (Scion Image; Scion Corporation, Frederick, MD).

Immunohistochemical Localization of CRFR1. HEK293 cells were grown on polylysine-coated sterile coverslips, and then they were fixed in PBS containing 4% sucrose and 4% paraformaldehyde for 20 min at 4°C. The fixed cells were washed three times with PBS before permeabilization in PBS containing 0.1% Triton X-100 for 5 min. Blockade was then carried out with 4% horse serum in PBS for 1 h. This was followed by incubation in primary antibody (goat anti-CRFR1, 1:500; Santa Cruz Biotechnology, Inc.) for 1 h at 25°C. After washing three times with PBS, Alexa Fluor 488 chicken anti-goat IgG (green) (Invitrogen) was applied to the samples at a dilution of 1:500. The immunolabeled cells were visualized using a laser-scanning confocal microscope (Fluoview BX61; Olympus, Tokyo, Japan). Negative controls, omitting each primary antibody, were performed in each case, and no significant immunolabelings were observed (data not shown).

Measurement of cAMP. To determine intracellular cAMP levels, 0.5 mM 3-isobutyl-1-methylxanthine, a cyclic nucleotide phosphodiesterase inhibitor, was added to each well 30 min before the addition of CRF, UCN, or astressin to prevent breakdown of accumulated cAMP.

After incubation with CRF or UCN for 10 min, cells were immediately immersed in 0.25 ml of 0.1 M HCl to stop the reaction. For experiments using antagonist, the astressin was applied for 30 min before the 10-min incubation as described above. Cells were collected and then centrifuged at 3000 rpm for 15 min at room temperature. The intracellular cAMP content was determined from the supernatant using the direct cAMP enzyme immunoassay kit in accordance with the manufacturer's high-sensitivity acetylation protocol (Sigma-Aldrich).

Cloning of Rat CRFR1 Receptor. Rat CRFR1 mRNA was isolated from rat (Wistar) brain, and RT-PCR was performed using CRFR1 forward (5-ATGGGACGGCGCCCGCAGCTCCGGCTCG-3) and reverse (5-TCACACTGCTGTGGACTGCTTGATGC-3) primers. The PCR product was cloned into pGEM-T Easy (Promega, Madison, WI) vector, and the identity of the rat CRFR1 was confirmed by DNA sequencing. The full-length rat CRFR1 digested with restriction enzymes SpeI and NotI was subcloned into MCS B site of the pIRES vector (Clontech), whereas mCherry (gift from Dr. Roger Y. Tsien, University of California, San Diego, CA) was cloned into the MCS A site using the XhoI and EcoRI restriction enzyme sites.

Electrophysiological Recordings and Data Analysis. Whole-cell currents were recorded at room temperature. Extracellular solution contained 140 mM tetraethylammonium methanesulfonate, 10 mM HEPES, and 5 mM $BaCl_2$ (pH to 7.3 with CsOH). Patch pipettes (WPI, Sarasota, FL) have a resistance of 2 to 3 MΩ when filled with an internal solution of 138 mM Cs-$MeSO_3$, 5 mM CsCl, 0.5 EGTA, 1 mM $MgCl_2$, 4 mM MgATP, and 10 mM HEPES (pH 7.3, adjusted with CsOH). Complete replacement of external solution 2 ml/min in the chamber was achieved within 2 to 3 min. Whole-cell Ba^{2+} currents were recorded using a MultiClamp 700B amplifier (Axon Instruments, Foster City, CA), controlled and monitored with a PC running p-CLAMP software, version 9.3 (Axon Instruments). Series resistance was typically <5 MΩ, and then it was electronically compensated by at least 70%. Data were low pass-filtered at 2 kHz using the built-in Bessel filter of the amplifier, and subtraction of capacitance and leakage current was carried out on-line using the P/4 protocol. Student's t tests were used to compare the different values, and they were considered significant at $P < 0.05$. All data are expressed as means ± S.E.M., and GraphPad Prism software (GraphPad Software Inc., San Diego, CA) was used for data plotting. Concentration–response curves were fitted by sigmoidal Hill equation $I/I_{control} = 1/(1 + 10^{(\log IC_{50\text{-}X})n_H})$, where X is the decadic logarithm of the concentration used, IC_{50} is the concentration at which the half-maximum effect occurs, and n_H is the Hill coefficient. The current-voltage (I-V) curves were fitted by $I_{Ba} = G_{max}(V - E_{rev})/\{1 + \exp((V - V_{1/2})/k_{I\text{-}V})\}$. Activation data were fitted by $G/G_{max} = F_{low}/\{1 + \exp((V_{1/2,low} - V)/k_{low})\} + (1 - F_{low})/\{1 + \exp((V_{1/2,high} - V)/k_{high})\}$, where $V_{1/2act}$ is the potential for half-activation calculated from dual Boltzmann functions when $G = 0.5\ G_{max}$. Steady-state inactivation data were fitted by a Boltzmann function of the form $I/I_{max} = (A1 - A2)/\{1 + \exp((V - V_{1/2inact})/k_{inact})\} + A2$. Recovery of currents from inactivation was tested using a double-pulse protocol. The peak current from the second test pulse was always normalized to the first 1-s pulse, and the plot of normalized current versus repolarization time was fitted with a double exponential equation: $Y = Y_{min} + A_1 \times [1 - \exp(-t/\tau_f)] + A_2 \times [1 - \exp(-t/\tau_s)]$, where Y is the fraction of recovery, A_1 and A_2 are the maximum values of the fast and slow component, and τ_f and τ_s are the time constants, respectively.

Pharmacological Agents. All drugs were obtained from Sigma-Aldrich, unless otherwise indicated. Stock solutions of UCN, CRF, PKI 5-24, chelerythrine chloride, pertussis toxin (PTX), cholera toxin (CTX), and astressin were prepared in distilled deionized water. Stock solutions of GF109203X, H-89, wortmannin, genistein, KN-93, and U-73122 were prepared in dimethyl sulfoxide. The concentration of dimethyl sulfoxide in the bath solution is expected to be less than 0.01%, and it had no functional effects on the T-type calcium currents. The QEHA peptide (QEHAQEPERQYMHIGTMVEFAYALVGK) and SKEE peptide (SKEEKSDKERWQHL ADLADFALAMKDT) were synthesized by GenScript Corporation (Scotch Plains, NJ). The peptides were purified by high-performance liquid chromatography (>95%), and the identities were verified by mass spectrometry.

Results

HEK293 Cells Endogenously Expressed Functional CRFR1. Previous reports have shown that HEK293 cells endogenously express CRF receptors (Dautzenberg et al., 2000). To confirm both the receptor subtype and the ability of endogenous receptors to transduce downstream signals after binding CRF or UCN, we characterized HEK293 cells by RT-PCR, Western blot, and immunohistochemistry analyses.

RT-PCR analysis demonstrated that CRFR1 mRNA was expressed in HEK293 cells, but that neither CRFR2α nor CRFR2β mRNA could be detected (Fig. 1A). As controls for the RT-PCR, CRFR2α and CRFR2β transcripts could be clearly amplified from mRNAs isolated from mouse hypothalamus and left atrium, respectively (Fig. 1A). All RT-PCR reactions were able to amplify β-actin, whereas the negative controls performed in parallel in the absence of reverse transcriptase enzyme in the RT reaction showed no product. Western blot analysis of HEK293 cell protein lysates using anti-CRFR1 antibody revealed that CRFR1 was expressed at the predicted size of ~55 kDa, whereas CRFR2 was not detected by anti-CRFR2 antibody (Fig. 1B). As a positive control, mouse hypothalamus, which is known to express both CRFR1 and CRFR2, showed prominent bands of ~55 kDa (CRFR1) and ~65 kDa (CRFR2), and both HEK293 cell and hypothalamus lysates produced robust staining for β-actin (Fig. 1B). As CRF receptors belong to the family of seven-transmembrane GPCRs (Markovic et al., 2006) and would be expected to be localized to the plasma membrane, we examined the distribution of CRFR1 on HEK293 cells by confocal microscopy. Figure 1C clearly shows the membrane localization of CRFR1. To test the functionality of the endogenous CFRR1 in HEK293 cells, we measured the levels of cAMP produced from CRFR1 activation by either CRF or UCN, both of which are known to activate adenylate cyclase (Markovic et al., 2006). Upon either 0.01 μM CRF or 0.01 μM UCN application to HEK293 cells, cAMP production was stimulated ~7-fold over basal levels (Fig. 1D). In the presence of the CRFR1 antagonist, 1 μM astressin, the stimulation of cAMP accumulation by UCN or CRF was completely abrogated (Fig. 1D). Taken together, the results show that the HEK293 cells endogenously expressed fully functional CRFR1 and that they could therefore be used to investigate the mechanisms by which Ca_V3 T-type calcium channels might be affected.

CRFR1 Selectively Inhibited $Ca_V3.2$ T-Type Calcium Channels. The binding affinities of CRF and UCN peptides to CRFR1 are roughly similar (Dautzenberg et al., 2000), and we decided to first investigate the activation of CRFR1 by UCN on Ca_V3 T-type calcium channels. Figure 1 shows that rat $Ca_V3.2$ channels were selectively inhibited by application of 0.1 μM UCN, whereas the rat $Ca_V3.1$ and $Ca_V3.3$ T-type calcium channels were not affected. A similar selective inhibition of $Ca_V3.2$ channels was observed at all test potentials (Fig. 2, A–C, right). Overall, application of 0.1 μM UCN significantly reduced $Ca_V3.2$ currents by ~31% ($I/I_{control}$ = 0.70 ± 0.05, n = 15, $P < 0.05$), whereas neither $Ca_V3.1$ nor $Ca_V3.3$ currents were significantly affected ($Ca_V3.1$: $I/I_{control}$ = 0.98 ± 0.03, n = 13, $P > 0.05$; $Ca_V3.3$: $I/I_{control}$ =

0.96 ± 0.04, $n = 6$, $P > 0.05$). After washout, $Ca_V3.2$ channel currents returned to baseline levels within 5 min (Fig. 2F), indicating the effect of UCN on $Ca_V3.2$ currents was not due to rundown. To determine whether the observed selective inhibition of Ca_V3 was species-specific, we further investigated the effects of 0.1 μM UCN on the three human brain Ca_V3 T-type calcium channel isoforms expressed in HEK293 cells. Figure 1E shows a similar degree of UCN-mediated inhibition (~37%) of human $Ca_V3.2$ currents ($I/I_{control}$ = 0.63 ± 0.06, $n = 7$, $P < 0.01$), with no significant effects on either $Ca_V3.1$ ($I/I_{control}$ = 0.97 ± 0.03, $n = 9$, $P > 0.05$) or $Ca_V3.3$ ($I/I_{control}$ = 0.98 ± 0.07, $n = 7$, $P > 0.05$) currents. Electrophysiological recordings for the UCN-mediated inhibition of human Ca_V3 T-type calcium channels and the time course of the inhibition are shown (Supplemental Fig. 8).

CRFR1 Activation Affected $Ca_V3.2$ Channels by Shifting Steady-State Inactivation Properties. Before investigating the mechanism for the selective inhibition of $Ca_V3.2$ calcium channels via UCN activation of CRFR1, we examined 1) whether the response is dosage-dependent and 2) whether channel electrophysiological properties were affected. To address the first issue, we performed a UCN dose-response study for the inhibition of $Ca_V3.2$ currents. At a holding potential of −110 mV, application of UCN at 0.01, 0.1, 1, and 10 μM increasingly inhibited $Ca_V3.2$ currents by 15% ($I/I_{control}$ = 0.85 ± 0.03, $n = 8$, $P < 0.05$), 31% ($I/I_{control}$ = 0.70 ± 0.05, $n = 15$, $P < 0.05$), 41% ($I/I_{control}$ = 0.59 ± 0.04, $n = 9$, $P < 0.01$), and 43% ($I/I_{control}$ = 0.57 ± 0.05, $n = 7$, $P < 0.01$), respectively (Fig. 3A). The maximum inhibition reduced the original peak current by ~43%, with a calculated IC_{50} = 30.41 nM and a Hill coefficient = 0.98. We next evaluated the inhibition of UCN at a more physiological holding potential of −80 mV, and we found that the $Ca_V3.2$ channels were even more sensitive to inhibition by UCN with an ~4-fold decrease in the IC_{50} to 6.93 nM (Hill coefficient of 0.97; Fig. 3B). To address the second point, we investigated

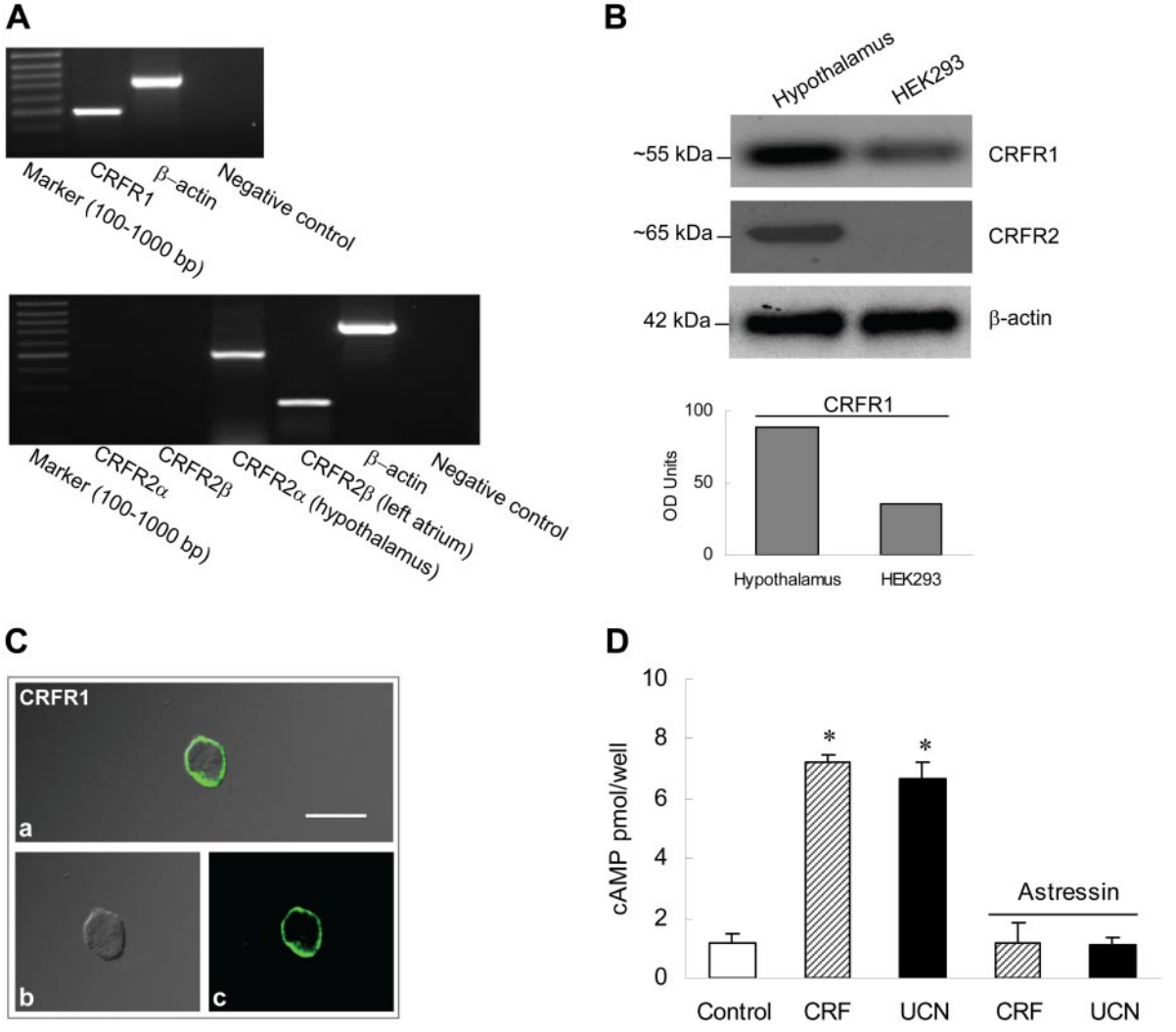

Fig. 1. CRFR1 is endogenously expressed in HEK293 cells. A, detection of CRFR1, CRFR2α, and CRFR2β in HEK293 cells. Total RNA from mouse hypothalamus or left atrium was used as positive controls for CRFR2α and CRFR2β, respectively. Negative control indicates RT-PCR reaction without the addition of RT. B, Western blot analysis of CRFR1 (top), CRFR2 (middle), and β-actin (bottom) of HEK293 membrane protein extracts. Mouse hypothalamus expressing both CRFR1 (~55 kDa) and CRFR2 (~65 kDa) is used as positive control, whereas β-actin expression controls for loading. Quantifications of band intensities are measures of relative expression levels. C, membrane expression of CRFR1 determined by confocal microscopy. Merged picture (top) of bright field (bottom, left) and fluorescent signals of CRFR1 (bottom, right). Scale bar, 20 μm. Proteins were immunolabeled by a monoclonal goat anti-CRFR1 antibody (green; Alexa). D, application of 0.01 μM UCN and 0.01 μM CRF stimulated robust cAMP production, but not in the presence of antagonist astressin at 1 μM. The results are representative of three independent experiments. *, $P < 0.05$ versus control.

whether the steady-state activation and inactivation properties of $Ca_V3.2$ channels were affected by bath application of 0.1 μM UCN. We observed a slight but statistically insignificant shift of 2 mV in the hyperpolarizing direction of the activation potential ($V_{1/2}$ from -41.8 ± 2.6 to -43.7 ± 1.3 mV and k value from 5.9 ± 0.3 to 6.0 ± 0.6, $n = 19$, $P > 0.05$) (Fig. 3C). In contrast, 0.1 μM UCN significantly shifted the steady-state inactivation potentials of $Ca_V3.2$ calcium channels in the hyperpolarizing direction by ~13 mV ($V_{1/2}$ from -66.7 ± 0.6 to -79.5 ± 0.7 mV, and k value from 4.9 ± 0.6 to 7.2 ± 0.7, $n = 17$, $P < 0.05$) (Fig. 3D). In addition, UCN at 30 nM (~IC_{50} at holding potential of -110 mV) shifted the steady-state inactivation potentials of $Ca_V3.2$ calcium channels in the hyperpolarizing direction by an expected smaller

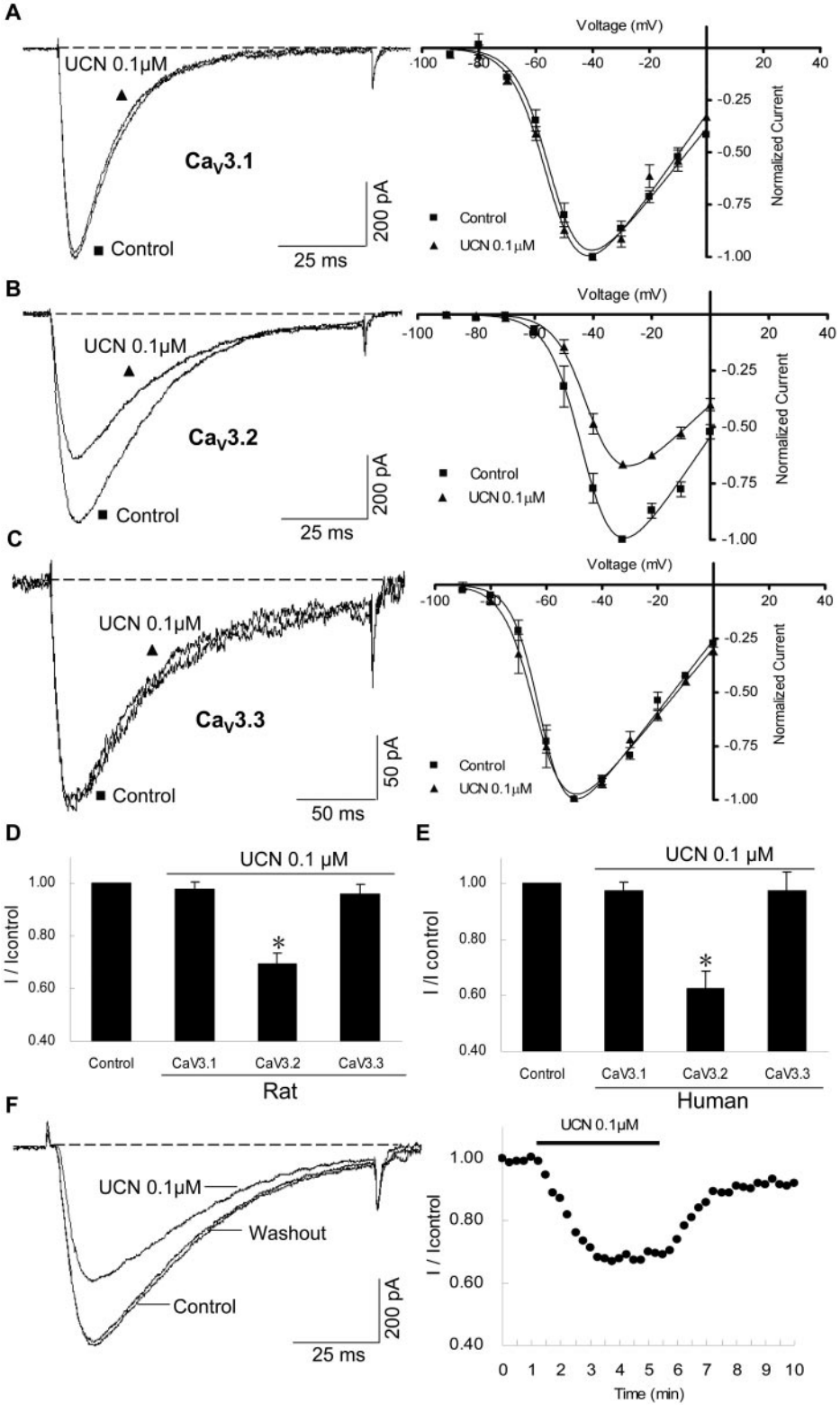

Fig. 2. Effects of UCN-mediated CRFR1 activation on cloned T-type Ca_V3 calcium channels. A to C, left, representative traces showing the effect of 0.1 μM UCN (black triangles) on 5 mM Ba^{2+} currents elicited by a -30-mV test pulse. Right, I-V profiles (evoked by a series of depolarizing pulses from a holding potential of -110 mV to test potentials between -90 and 0 mV, in 10-mV increments) obtained for cloned rat $Ca_V3.1$ (A; $n = 13$), $Ca_V3.2$ (B; $n = 15$), and $Ca_V3.3$ subunits (C; $n = 6$). D, effect of 0.1 μM UCN on I_{Ba} flowing through cloned rat $Ca_V3.1$, $Ca_V3.2$, and $Ca_V3.3$ channels elicited by a -30-mV test pulse. E, effect of 0.1 μM UCN on I_{Ba} flowing through cloned human $Ca_V3.1$ ($n = 9$), $Ca_V3.2$ ($n = 7$), and $Ca_V3.3$ ($n = 7$) channels elicited by a -30-mV test pulse. F, exemplary traces (left) and time course (right) of $Ca_V3.2$ currents obtained before (control), during, and after (washout) the application of 0.1 μM UCN. After washout, $Ca_V3.2$ currents recorded in control cells returned to original amplitude.

potential of ~8 mV ($V_{1/2}$ = −75.3 ± 0.7 mV and k = 6.6 ± 0.8, n = 6, $P < 0.05$ versus control) (Fig. 3E), suggesting a dose dependence in the shift of the steady-state inactivation upon activation of CRFR1 by UCN. Furthermore, after 0.1 μM UCN washout, the steady-state inactivation reversed to values similar to controls before UCN application ($V_{1/2}$ = −68.4 ± 0.7 and k = 5.2 ± 0.6, n = 8, $P < 0.05$). This result suggests that the reduction in $Ca_V3.2$ currents observed upon application of UCN could be the result of increased channels remaining in the inactivated state. We further determined whether activation of CRFR1 will affect $Ca_V3.2$ recovery from inactivation. A typical two-pulse protocol was used with a prepulse of 1-s duration (Fig. 3F). We observed a slight but statistically insignificant effect of 0.1 μM UCN ($P > 0.05$) on the fast and slow components of recovery from inactivation (control: τ_{fast} = 110 ± 19 ms, n = 9, τ_{slow} = 916 ± 113 ms, n =

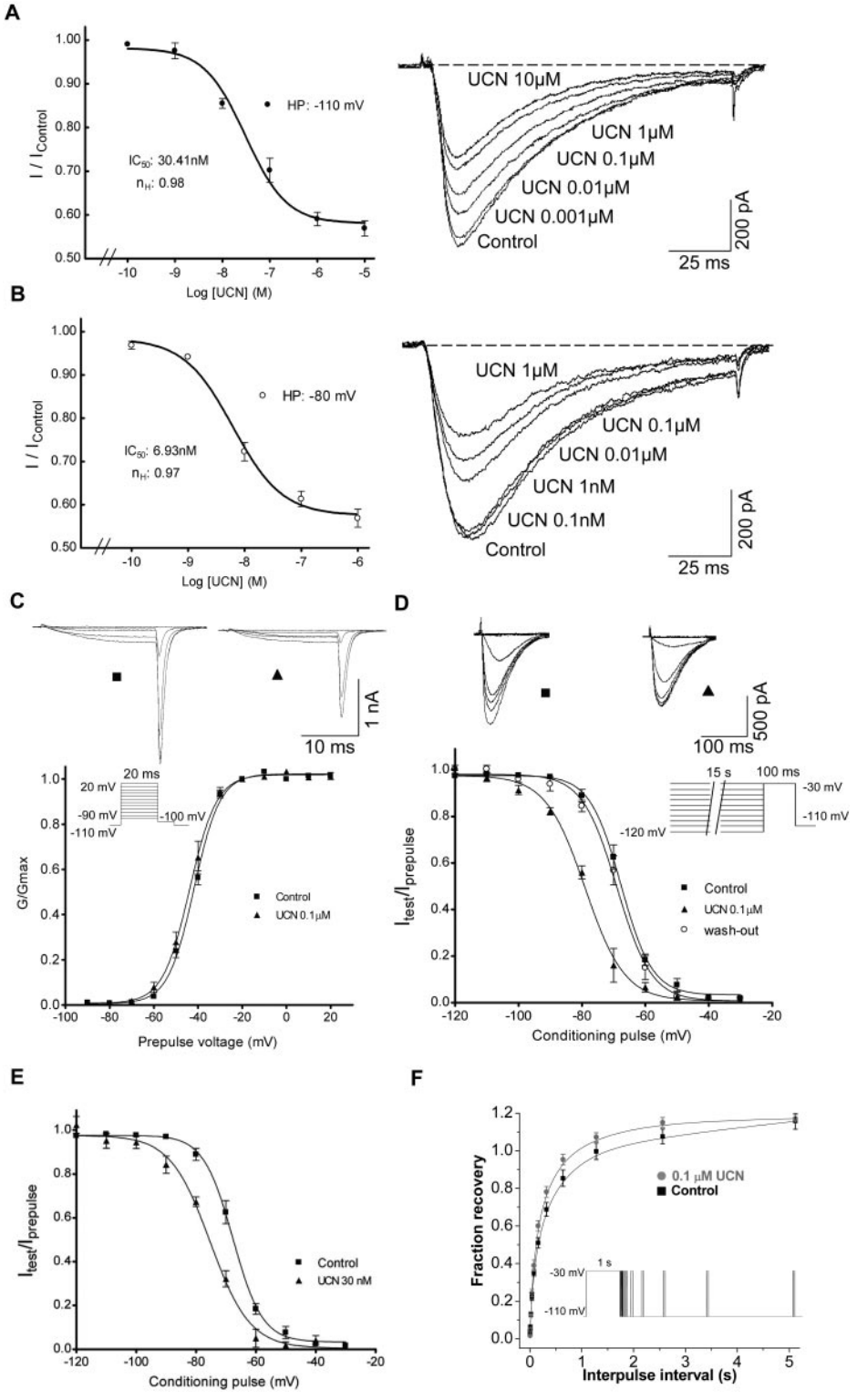

Fig. 3. Dose response and effects of UCN on $Ca_V3.2$ channel biophysical properties. A and B, concentration-dependent effects of UCN on $Ca_V3.2$ currents. $Ca_V3.2$ currents were evoked by a 100-ms depolarizing step to −30 mV from a holding potential of −110 mV (A) and −80 mV (B). Dose-response curves were established by fitting the normalized currents with a sigmoidal Hill equation, where $I/I_{control} = 1/(1 + 10^{(\log IC_{50\text{-}[supi]X})n_H})$ (left; see Supplemental Material). Exemplary traces in the absence and presence of UCN on evoked $Ca_V3.2$ currents are shown (right). C, effects of 0.1 μM UCN on the steady-state activation curve of $Ca_V3.2$. Exemplary tail currents evoked by repolarizations to −100 mV after depolarizing test pulses at −90, −60, 0, or 20 mV (top) and normalized steady-state activation curves (bottom) in the absence (■) and presence (▲) of UCN. Steady-state activation curves were activated by a variant voltage family of 20-ms test pulses, from −90 to 20 mV, and tail currents were recorded on repolarization to −100 mV. D, effect of 0.1 μM UCN on the steady-state inactivation curve of $Ca_V3.2$. Typical current traces after 15-s conditioning depolarizing pulses evoked at −120, −90, −60, or −30 mV (top) and normalized steady-state inactivation curves (bottom) in the absence (■) and presence (▲) of UCN, and washout (O). Steady-state inactivation curves were obtained by evoking $Ca_V3.2$ currents with a test depolarization to −30 mV applied at the end of 15-s conditioning pulses ranging from −120 to −30 mV. E, effect of 30 nM UCN on the steady-state inactivation of $Ca_V3.2$ (n = 6). F, effect of 0.1 μM UCN on the recovery from inactivation of $Ca_V3.2$ channels. Double-pulse protocol started from a holding potential of −110 mV, with a 1-s depolarizing prepulse to −30 mV, following by a variable length (from 10 ms to 5.12 s) of repolarization to −110 mV, and finally a second 50-ms depolarizing pulse to −30 mV. Sweeps were separated by 20 s to allow for complete channel recovery. Fraction recovery was calculated as the ratio of the peak current measured during the second test pulse divided by the peak current measured during the prepulse.

9; 0.1 μM UCN: τ_{fast} = 103 ± 17 ms, n = 9, τ_{slow} = 684 ± 72 ms, n = 9) (Fig. 3F), which suggested that the UCN blockade purely shifted the steady state of inactivation potentials to the left and that it did not affect the rate of recovery. Interestingly, however, there seemed to be some facilitation of the $Ca_V3.2$ channels under both conditions.

UCN and CRF Similarly Inhibited $Ca_V3.2$ Currents by Activation of CRFR1. To confirm that the UCN-mediated response occurred via CRFR1, we examined its effects on $Ca_V3.2$ currents in the presence or absence of the CRFR antagonist astressin. Preincubation with 1 μM astressin blocked the UCN-induced inhibition ($I/I_{control}$ = 0.95 ± 0.06, n = 6, $P < 0.05$) (Fig. 4A), indicating that the inhibition of $Ca_V3.2$ channels is CRFR1-dependent. Importantly, CRF peptide activation of CRFR1 also showed robust inhibition (by ~28%) of the $Ca_V3.2$ currents ($I/I_{control}$ = 0.72 ± 0.04, n = 6, $P < 0.05$) (Fig. 4B) and was CRFR1-dependent as demonstrated by the abrogation of inhibition after preincubation with 1 μM astressin.

$Ca_V3.2$ Channel Inhibition Can Be Enhanced by Exogenous CRFR1 Expression. We next explored whether augmentation of CRFR1 levels through the overexpression of cloned CRFR1 in HEK293 cells could affect the degree of inhibition of $Ca_V3.2$ channels mediated by UCN or CRF. We first cloned and then characterized the rat CRFR1 in HEK293 cells. Western blot analysis of CRFR1 proteins isolated from mouse hypothalamus and CRFR1-transfected HEK293 lysates showed a predominant ~55-kDa band stained by anti-CRFR1 (Fig. 5A). The total amount of CRFR1 protein expressed in the HEK293 cells after transient transfection with cloned CRFR1 showed a 3- to 4-fold increase over the endogenous level, after normalization with the β-actin expression level (Figs. 1B and 5A). Application of 0.01 μM UCN or 0.01 μM CRF on HEK293 cells transfected with the cloned CRFR1 stimulated cAMP production by approximately 80-fold over basal levels (82.91 ± 6.40 for CRF and 79.29 ± 6.37 for UCN). This represented an ~10-fold increase in cAMP compared with that for nontransfected HEK293 cells (Figs. 1D and 5B). In the presence of the CRFR1 antagonist astressin at 1 μM, the level of cAMP production after application of either UCN or CRF was not significantly different from basal level exhibited by control HEK293 cells (Fig. 5B).

We also examined whether the level of $Ca_V3.2$ channel inhibition might be increased in the CRFR1-transfected HEK293 cells. Figure 5C shows that upon application of either 0.1 μM UCN or CRF that $Ca_V3.2$ currents were significantly reduced by 46.3% ($I/I_{control}$ = 0.54 ± 0.04, n = 6, $P < 0.05$) and 42.5% ($I/I_{control}$ = 0.57 ± 0.04, n = 6, $P < 0.05$), respectively. These values represent an ~50% increase in the degree of inhibition of $Ca_V3.2$ currents compared with that for non–CRFR1-transfected HEK293 cells. Dose-response analysis of UCN inhibition in CRFR1 transfected HEK293 cells showed an enhanced affinity by ~6-fold (IC_{50} = 5.07 nM and Hill coefficient = 0.96) (Fig. 5C, bottom). Again, pretreatment of the cells with 1 μM astressin abrogated the inhibitory effects of UCN and CRF on $Ca_V3.2$ currents ($I/I_{control}$ = 0.95 ± 0.03 for UCN, n = 6 and $I/I_{control}$ = 0.96 ± 0.04 for CRF, n = 6) (Fig. 5, C and D). Overall, the apparent nonlinearity of the relationship between the level of CRFR1 protein, the production of cAMP, and the degree of $Ca_V3.2$ inhibition may reflect the fact that cAMP/cAMP-dependent protein kinase (PKA)-dependent intracellular signaling factors required to affect inhibition of $Ca_V3.2$ channels might be lim-

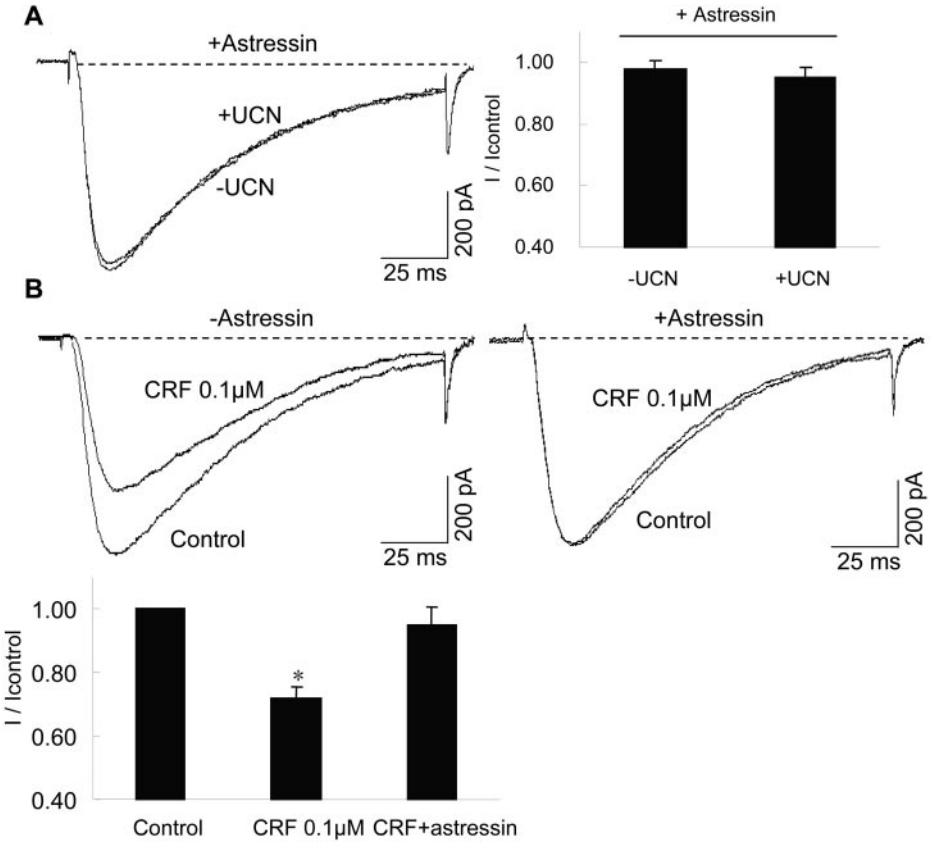

Fig. 4. UCN and CRF inhibit $Ca_V3.2$ currents via activation of CRFR1. $Ca_V3.2$ currents were evoked by a 100-ms depolarizing step to −30 mV from a holding potential of −110 mV. Cells were incubated with 1 μM astressin for 30 min before application of UCN or CRF. A, exemplary traces (left) and pooled data (right) show the effects of 0.1 μM UCN on $Ca_V3.2$ currents in the presence of 1 μM astressin. B, exemplary traces (top) and pooled data (bottom) show the effects of 0.1 μM CRF on $Ca_V3.2$ currents in the absence (left) and presence (right) of astressin.

iting. Alternatively, it may indicate that a signaling mechanism distinct from the well described CRFR1-mediated cAMP/PKA pathway is involved in the inhibition of $Ca_V3.2$ T-type channels (see below).

Involvement of G Proteins in CRFR1-Mediated $Ca_V3.2$ Calcium Channel Inhibition. To address whether G proteins are directly involved in the CRFR1-dependent inhibition of $Ca_V3.2$ calcium channels, we dialyzed into cells guanosine-5′-*O*-(2-thiodiphosphate) (GDPβS; 1 mM), a non-hydrolysable GDP analog. It shows that GDPβS abolished the inhibition of $Ca_V3.2$ currents by 0.1 μM UCN (Fig. 6A, left; $I/I_{control} = 0.97 \pm 0.03$, $n = 6$). In contrast, the nonhydrolyzable GTP analog guanosine-5′-*O*-(3-thiotriphosphate) (GTPγS; 100 μM) did not prevent the UCN-mediated inhibition of $Ca_V3.2$ currents ($I/I_{control} = 0.58 \pm 0.03$, $n = 6$, $P < 0.05$) and that the inhibition remained for up to 10 min after the washout of UCN. For control cells not dialyzed with intracellular GTPγS, the inhibition by UCN was reversed and the currents returned to baseline levels within 5 min after the washout of UCN (Fig. 6B). These results indicated

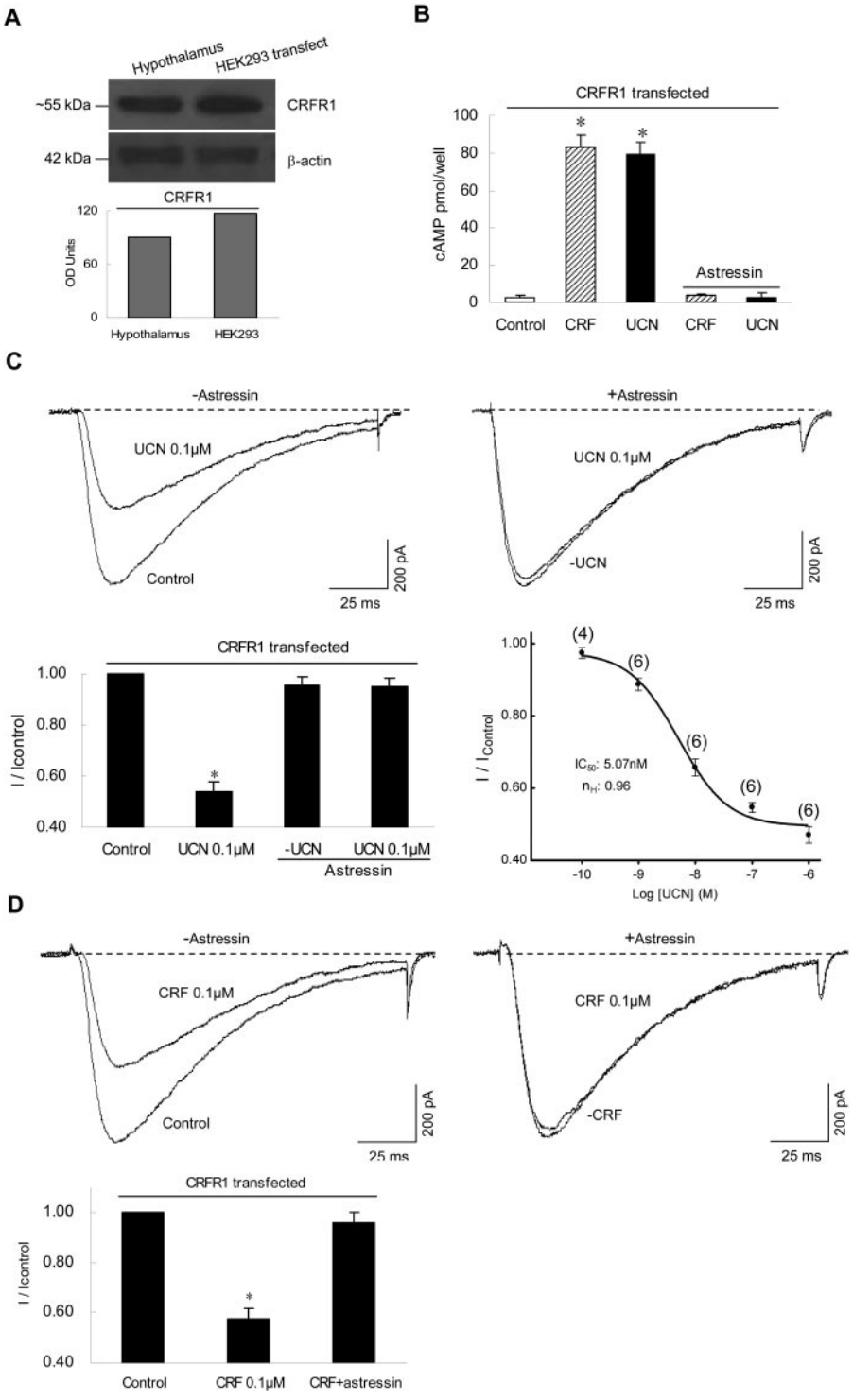

Fig. 5. Effects of overexpression of CRFR1 on $Ca_V3.2$ channels. A, Western blot analysis showed robust expression of cloned CRFR1 transfected in HEK293 cells. Anti-CRFR1 immunolabeled mouse hypothalamus (left lane, positive control) and transfected HEK293 cells (right lane) showing the ~55-kDa CRFR1, with β-actin as control (42 kDa, bottom). B, stimulation of cAMP in CRFR1-transfected HEK293 cells by 0.01 μM CRF ($n = 6$), 0.01 μM UCN ($n = 6$) in the presence or absence of 1 μM astressin ($n = 6$). The results are from three independent experiments done in duplicates; *, $P < 0.05$ versus control. C and D, effects of UCN (C) ($n = 6$) and CRF (D) ($n = 6$) on $Ca_V3.2$ currents in HEK293 cells cotransfected with $Ca_V3.2$ and CRFR1 cDNA. Exemplary traces show the effects of 0.1 μM UCN or 0.1 μM CRF on $Ca_V3.2$ currents in the absence (top, left) ($n = 6$) and presence (top, right) ($n = 6$) of 1 μM astressin. Pooled data are shown as mean ± S.E.M. for control and drug treated cells (bottom, left). Dose-response curves were fitted by a sigmoidal Hill equation. $Ca_V3.2$ currents were evoked by a 100-ms depolarizing step to −30 mV from a holding potential of −110 mV. Astressin alone did not affect the amplitudes of $Ca_V3.2$ currents (C; bottom, $n = 6$), *, $P < 0.05$ versus control.

that G proteins are involved in the CRFR1-mediated inhibition of $Ca_V3.2$ currents. We further determine that which isoform of Gα was involved in this inhibition. To investigate whether the UCN-mediated response occurred via Gα_s, we examined its effects on $Ca_V3.2$ currents in the presence of CTX, which could catalyze ADP-ribosylation of Gα_s. Pretreatment of $Ca_V3.2$-expressing cells with CTX (500 ng/ml for 24 h) abolished the UCN-induced inhibition ($I/I_{control}$ = 0.95 ± 0.06, n = 6) (Fig. 6C), indicating that the inhibition of $Ca_V3.2$ channels is Gα_s-dependent. In addition, after pretreatment of the cells with PTX (200 ng/ml for 24 h), which catalyzes the ADP-ribosylation of G$\alpha_{i/o}$, UCN still mediated robust inhibition of the $Ca_V3.2$ currents ($I/I_{control}$ = 0.67 ± 0.07, n = 5) (Fig. 6C). The $Ca_V3.2$ currents inhibition induced by CRFR1 activation was sensitive to CTX but not PTX, implicating Gα_s, instead of G$\alpha_{i/o}$, was involved. As CTX activated Gα_s, we also examined whether CTX would by itself trigger a shift in half-inactivation potential compared with control cells. In CTX-treated cells, we observed a significant shift of ~10 mV in the hyperpolarizing direction of the inactivation potential (66.7 ± 0.6 to −76.8 ± 0.9 mV and k from 4.9 ± 0.6 to 6.5 ± 0.8, n = 6, $P < 0.05$) (Fig. 6D). To further test whether UCN-mediated $Ca_V3.2$ currents inhibition proceeds through a G$\alpha_{q/11}$-mediated pathway, $Ca_V3.2$ currents inhibition was examined in the presence of 0.1 μg/μl RGS2, which could selectively bind G$\alpha_{q/11}$-GTP (Kammermeier and Ikeda, 1999). In RGS2-expressing cells, UCN still inhibited $Ca_V3.2$ currents by ~29% ($I/I_{control}$ = 0.70 ± 0.02, n = 5) (Fig. 6C), which is not significantly different compared with the RGS2-nontransfected cells. These results suggested that Gα_s, not G$\alpha_{i/o}$ and G$\alpha_{q/11}$, is involved in the UCN-induced $Ca_V3.2$ channels inhibition.

UCN Inhibited $Ca_V3.2$ Channels Independently of Phospholipase C and Downstream Protein Kinases. Previous reports have shown that cardiovascular and neuronal protections by UCN are mediated via activation of either cAMP/PKA or PKC (Markovic et al., 2006). As it has also been reported that T-type calcium channels can be regulated by serine-threonine kinases, tyrosine kinases (TK), and phospholipase C (PLC) pathways (Chemin et al., 2006), we investigated whether the inhibitory effects of CRFR1 are mediated by these known pathways. After pretreatment of $Ca_V3.2$-expressing cells with the selective PKC inhibitors GF109203X (1 μM) or chelerythrine chloride (1 μM), 0.1 μM UCN still mediated robust inhibition of the $Ca_V3.2$ currents ($I/I_{control}$ = 0.70 ± 0.04, n = 6, $P < 0.05$ versus control and $I/I_{control}$ = 0.70 ± 0.08, n = 5, $P < 0.05$ versus control, respectively) (Fig. 7, A and G). Likewise, pretreatment with selective PLC inhibitors U-73122 (3 μM) (Suh and Hille, 2002) or ET-18-OCH_3 (10 μM), did not prevent the inhibition of $Ca_V3.2$ currents by UCN ($I/I_{control}$ = 0.67 ± 0.03, n = 5, $P < 0.05$ versus control and $I/I_{control}$ = 0.68 ± 0.05, n = 5, $P < 0.05$ versus control, respectively) (Fig. 7, B and G). The degree of inhibition by UCN in the presence or absence of

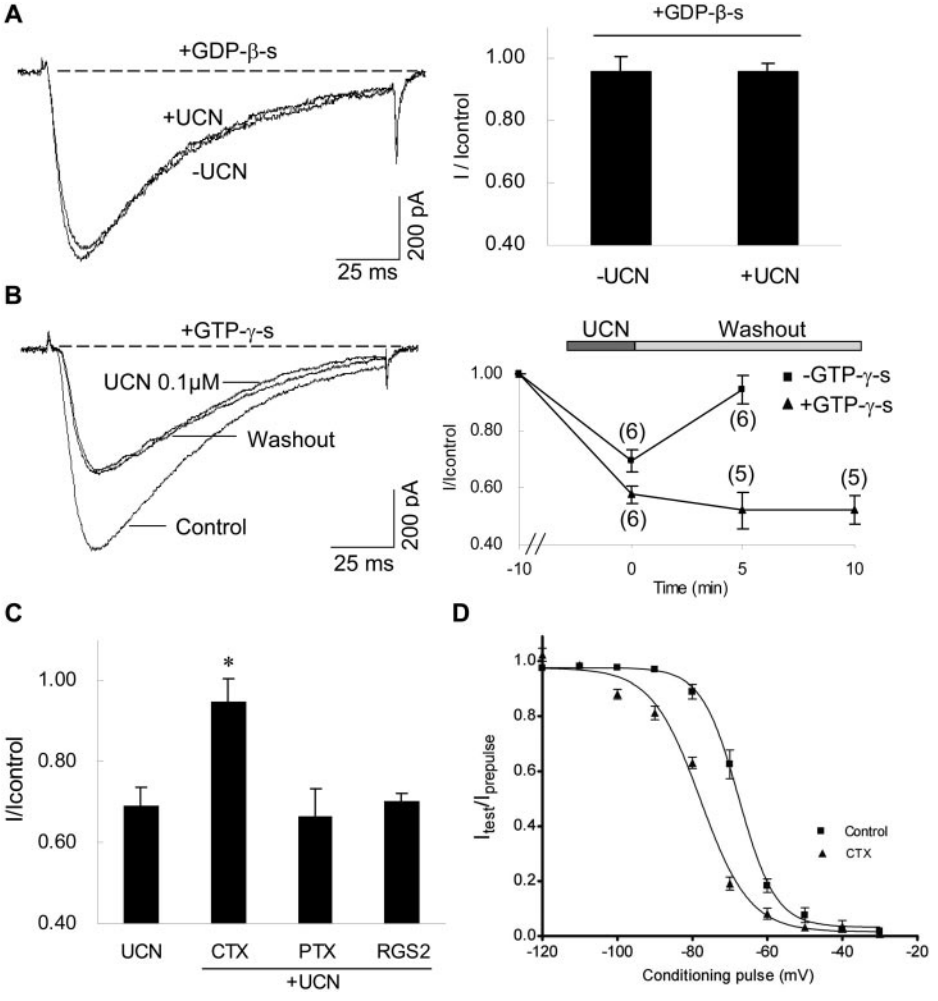

Fig. 6. G protein-mediated inhibition of $Ca_V3.2$ channels by UCN. A, exemplary traces of $Ca_V3.2$ currents before (−UCN) and during 0.1 μM UCN (+UCN) application in the presence of 1 mM GDPβS (left). Pooled data show the mean current amplitude ± S.E.M. of $Ca_V3.2$ currents (n = 6). B, time course of UCN inhibition on $Ca_V3.2$ currents in absence and presence of GTPγS. Exemplary traces of $Ca_V3.2$ currents obtained in presence (left) of GTPγS, before, during, and after washout of the application of 0.1 μM UCN. Application of UCN (dark bar, bottom) was for 5 min before washout for the next 10 min (light bar). Both control cells (■) and cells recorded with 0.1 mM GTPγS in the patch pipette (▲) show current inhibition as evaluated at time = 0 min. After washout, $Ca_V3.2$ currents recorded in control cells, in the absence of GTPγS, returned to original amplitude, whereas GTPγS-treated cells show a continuous inhibition for up to 10 min. Numbers in parentheses indicate number of cells tested. C, effects of UCN on $Ca_V3.2$ currents in PTX (200 ng/ml for 24 h, n = 5) or CTX (500 ng/ml for 24 h, n = 5)-pretreated cells, and RGS2-expressing HEK293 cells (0.1 μg/μl, n = 5). $Ca_V3.2$ currents (A–C) were evoked by a 100-ms depolarizing step to −30 mV from a holding potential of −110 mV. D, effect of 500 ng/mL CTX on the steady-state inactivation curve of $Ca_V3.2$. Steady-state inactivation curves in the absence (■) or presence (▲) of CTX were obtained by evoking $Ca_V3.2$ currents with a test depolarization to −30 mV applied at the end of 15-s conditioning pulses ranging from −120 to −30 mV.

PKC inhibitors (GF109203X or chelerythrine chloride) and PLC inhibitors (U-73122 or ET-18-OCH_3) were not significantly different. After pretreatment with 100 μM genistein, a broad-spectrum inhibitor of TK, and after current amplitudes had stabilized, application of 0.1 μM UCN inhibited the I_{Ba} by ~27% ($I/I_{control}$ = 0.73 ± 0.06, n = 5) (Fig. 7C), which was not different from the inhibition obtained in the absence of genistein. Previous reports also showed that CaMKII and phosphatidylinositol 3-kinase (PI3K) were involved in G protein-mediated regulation of T-type calcium channels (Chemin et al., 2006). Here, preincubation with 1 μM wortmannin, a specific PI3K inhibitor, or 0.5 μM KN-93, a selective CaMKII inhibitor, failed to prevent the UCN-induced inhibition of $Ca_V3.2$ channel currents [$I/I_{control}$ = 0.69 ± 0.08, n = 5, $P < 0.05$ versus control) (Fig. 7D); $I/I_{control}$ = 0.65 ± 0.06, n = 5, $P < 0.05$ versus control (Fig. 7E)], indicating that the PI3K and CaMKII pathways were not involved. As activation of CRFR1 increases cAMP accumulation and PKA activity (Dautzenberg et al., 2002), blocking PKA activity might be expected to block the effect of UCN-mediated inhibition. To test this possibility, we dialyzed the cells with a pipette solution containing PKI 5-24 (1 μM) and found no effect on the $Ca_V3.2$ currents over 5 min. After this pretreatment of PKI 5-24 for 5 min, application of 0.1 μM UCN still reduced current amplitudes by 30% ($I/I_{control}$ = 0.70 ± 0.05, n = 6, $P < 0.05$ versus control) (Fig. 7F) similar to that for currents recorded in the absence of PKI 5-24. Similar inhibition by UCN on $Ca_V3.2$ currents with 0.5 μM H-89 (~29%; $I/I_{control}$ = 0.71 ± 0.07, $P < 0.05$ versus control, n = 5) was also obtained (Fig. 7G). Taken together, these results indicate that the inhibition of $Ca_V3.2$ currents mediated by CRFR1 is not likely to be mediated via PLC or downstream PKA, PKC, CaMKII, PI3K, or TK signaling pathways.

UCN Inhibited $Ca_V3.2$ T-Type Calcium Channels via G Protein $\beta\gamma$ Subunits. We further tested whether the UCN-induced inhibition of $Ca_V3.2$ currents might be mediated via G$\beta\gamma$ subunits by introducing into the recording pipette a synthetic peptide, QEHA (encoding residues 956 to 982 of adenylyl cyclase 2), which competitively binds G$\beta\gamma$

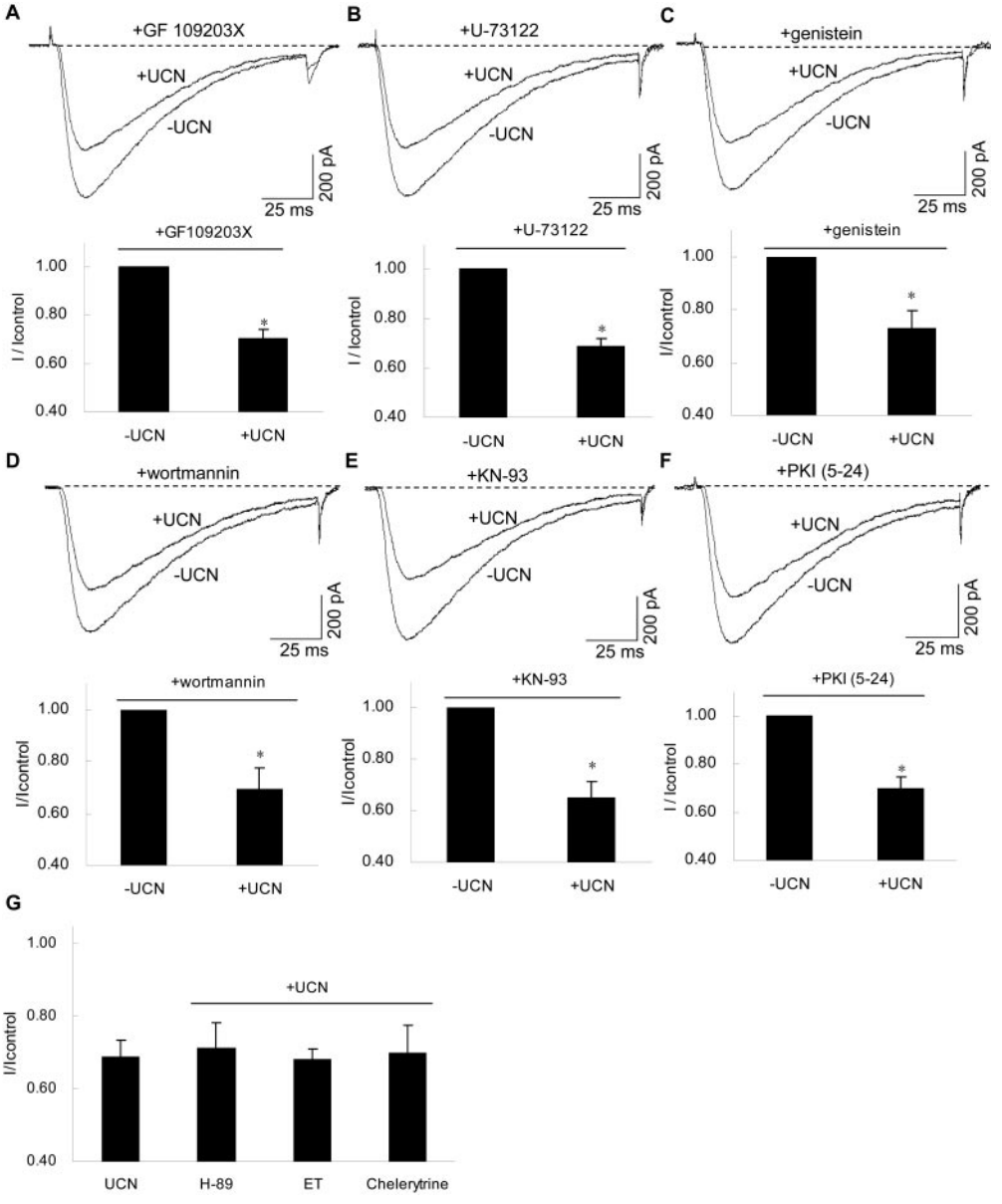

Fig. 7. UCN inhibits $Ca_V3.2$ channels independently of PKC, PKA, TK, PI3K, CaMKII, and PLC (A–G). $Ca_V3.2$ currents were evoked by a 100-ms depolarizing step to −30 mV from a holding potential of −110 mV. Cells were incubated with 1 μM GF109203X for 30 min (A; n = 6), 3 μM U-73122 for 30 min (B; n = 5), 100 μM genistein for 30 min (C; n = 5), 1 μM wortmannin (D; n = 5), and 0.5 μM KN-93 (E; n = 5), or intracellular applied 1 μM PKI 5-24 (F; n = 6). Pretreatment of cells with 0.5 μM H-89 (n = 5), 10 μM ET-18-OCH_3 (ET; n = 5), and 1 μM chelerythrine chloride (n = 5) is shown (G). The amplitude of the peak $Ca_V3.2$ current in the presence of UCN is normalized to the peak current recorded before drug application. Exemplary traces (A–F, top) and pooled data (A–F, bottom) show $Ca_V3.2$ currents in the absence (−UCN) or presence (+UCN) of 0.1 μM UCN. *, $P < 0.05$ versus control.

and blocks Gβγ-mediated signaling (Chemin et al., 2006). As a control, we used a synthetic SKEE peptide, representing the cognate region of adenylyl cyclase 3, that does not bind Gβγ. Our results showed that intracellular pipette application of 200 μM QEHA suppressed the effects of 0.1 μM UCN ($I/I_{control}$ = 0.97 ± 0.03, n = 6 for −UCN and 0.95 ± 0.04, n = 9 for +UCN) (Fig. 8, A and B). Furthermore, the intracellular application of the QEHA peptide also eliminated the hyperpolarizing shift in the steady-state inactivation potential normally elicited by UCN ($V_{1/2}$ = −69.6 ± 0.7 for control and $V_{1/2}$ = −67.8 ± 0.9 mV for UCN + QEHA, n = 5, P > 0.05) (Fig. 8E). In contrast, intracellular application of 200 μM SKEE peptide did not significantly affect the UCN-induced inhibition of $Ca_V3.2$ currents ($I/I_{control}$ = 0.97 ± 0.02, n = 6 for −UCN and 0.69 ± 0.04, n = 7 for +UCN) (Fig. 8, C and D). Beside intracellular application of QEHA, a membrane-associating C-terminal construct of a G protein-coupled receptor kinase that sequesters Gβγ (MAS-GRK3) was transfected into HEK293 cells to further determine whether Gβγ is involved in the inhibition of $Ca_V3.2$ currents. When MAS-GRK3 was coexpressed in $Ca_V3.2$-expressing HEK293 cells, the robust inhibition by UCN was almost eliminated ($I/I_{control}$ = 0.92 ± 0.09, n = 5) (Fig. 8G). These results demonstrate that $Ca_V3.2$ channel inhibition is mediated via a Gβγ-dependent mechanism upon the activation of the CRFR1.

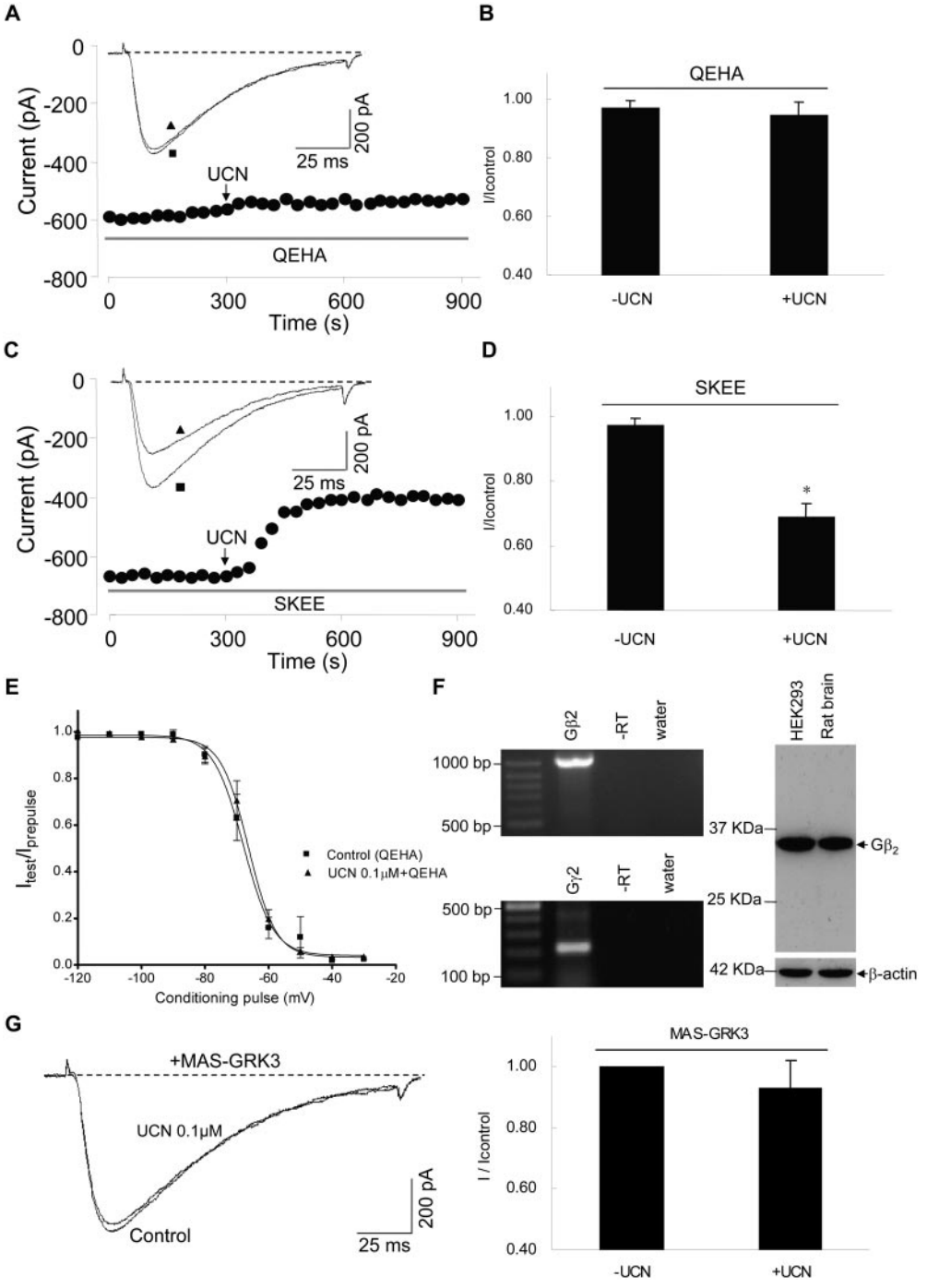

Fig. 8. Evidence that Gβγ mediates CRFR1-dependent inhibition of $Ca_V3.2$ currents. A, 200 μM synthetic QEHA peptide prevented current inhibition by 0.1 μM UCN perfused continuously as indicated by arrow. Inset, without UCN (■) and 0.1 μM UCN (▲). B, pooled data indicate QEHA peptide abolition of UCN-induced inhibition of $Ca_V3.2$ currents in the absence (−UCN, n = 6) or presence of 0.1 μM UCN (+UCN, n = 9). C, control 200 μM SKEE peptide did not prevent UCN-induced inhibition. Inset, without UCN (■) and +UCN (0.1 μM) (▲). D, pooled data indicate SKEE peptide effect on UCN-induced inhibition of $Ca_V3.2$ currents in the absence (−UCN, n = 6) and presence of 0.1 μM UCN (+UCN, n = 7); *, P < 0.05 versus control. E, steady-state inactivation curve of QEHA peptide in the absence of UCN (■) (n = 5) and presence of 0.1 μM UCN (n = 5) (▲). F, left, PCR products of $G_{\beta 2}$ (1023 base pairs) and $G_{\gamma 2}$ (216 base pairs) amplified from HEK293 mRNA. Negative controls: without adding RT (−RT) or template (water). Right, $G_{\beta 2}$ (top) was expressed in HEK293 cells and rat brain, with β-actin as control (bottom). G, effects of UCN on $Ca_V3.2$ currents in 0.01 μg/μl MAS-GRK3-coexpressed HEK293 cells (n = 5).

G protein-dependent inhibition of calcium channels has been previously demonstrated to require the $G_{\beta 2}$ subunit, whereas the requirement for a specific $G_{\gamma 2}$ subunit is less stringent (Wolfe et al., 2003). To support our results that the inhibition of $Ca_V3.2$ channels induced by CRFR1 activation was via $G\beta\gamma$, we investigated whether $G_{\beta 2}$ or $G_{\gamma 2}$ subunit was endogenously expressed in HEK293 cells. We found by RT-PCR that $G_{\beta 2}$ and $G_{\gamma 2}$ transcripts are endogenously expressed in HEK293 cells (Fig. 8F, left). Endogenous $G_{\beta 2}$ protein was also detected by anti-$G_{\beta 2}$ in HEK293 cells (Fig. 8F, right). Taken together, these results strongly suggest that native CRFR1 receptors couple via an endogenous $G\beta\gamma$-dependent signaling pathway to mediate the selective inhibition of $Ca_V3.2$ channels among the T-type subfamily of calcium channels. This pathway represents a novel CRFR1-coupled mechanism distinct from the previously described PLC and downstream kinase signaling pathways.

Discussion

CRF peptides mediate multiple physiological responses, including those involved in mammalian responses to stress and inflammation. There is also growing evidence that CRF peptides contribute toward human disorders such as anxiety, depression, and alcohol and drug addictions (Reul and Holsboer, 2002; Bale and Vale, 2004; Gravanis and Margioris, 2005, Bruijnzeel and Gold, 2005). Several CRF receptor subtypes are known to be expressed, and there is considerable interest in determining both the downstream effectors and mechanisms by which these GPCRs mediate their widespread physiological functions. In the present article, we demonstrate that activation of CRFR1 receptors by either CRF or UCN robustly inhibits $Ca_V3.2$ channels via a $G\beta\gamma$-dependent mechanism with no effect on either $Ca_V3.1$ or $Ca_V3.3$ T-type calcium channels. We also find that the CRFR1-mediated inhibition of $Ca_V3.2$ channels is state-dependent, likely occurring through stabilizing the channels in the inactivated state, and the inhibition is reversible after washout of UCN.

HEK293 cells are an appropriate expression system as these cells endogenously and exclusively express the corticotropin-releasing factor receptor 1, the CRFR1 subtype (Dautzenberg et al., 2000) (Fig. 1). Both the activation of endogenous and overexpressed cloned CRFR1 receptors produced robust and selective inhibition of cloned rat and human brain $Ca_V3.2$ T-type calcium channels. CRF and UCN have both been shown to bind CRFR1 receptors with similar affinities (Dautzenberg et al., 2000), and we found that $Ca_V3.2$ channel inhibition was also not ligand-dependent as both CRF and UCN elicited comparable levels of T-type calcium channels inhibition.

The G protein-dependent inhibition of T-type calcium channels has been previously demonstrated to require the $G_{\beta 2}$ subunit, whereas the requirement for a specific G_{γ} subunit is less stringent (Wolfe et al., 2003). These reports have found that inhibition mediated by G protein decreases the probability of opening of the $Ca_V3.2$ calcium channels, whereas activation and inactivation properties are unaltered. Note that, in our present findings, the activation of CRFR1 receptors by either CRF or UCN produced a distinct and significant hyperpolarizing shift in the steady-state inactivation potentials, whereas activation potentials remained unaltered. Unlike the activation of the dopamine receptor 1, which requires both cAMP and G protein to act in combination to inhibit T-type calcium currents (Drolet et al., 1997), a similar requirement was not evident for the CRFR1-mediated inhibition of the $Ca_V3.2$ channels. Evaluating the role of cAMP in CRFR1-mediated inhibition of $Ca_V3.2$ channels, application of PKI 5-24, a potent and selective peptide inhibitor of PKA, failed to diminish the inhibitory effects of CRFR1 activation, indicating that PKA is not directly involved in $Ca_V3.2$ inhibition.

Previous reports have shown that T-type calcium currents can also be modulated by the PKC signaling pathway. In one instance, examining GH3 cells showed that native T-type calcium currents are inhibited by 1-oleoyl-2-acetylglycerol (a diacylglycerol analog) (Herrington and Lingle, 1992). Similar results were reported for native T-type currents in chick dorsal root ganglion neurons, although in these neurons the direct inhibition was independent of PKC activation (Hockberger et al., 1989). Here, GF109203X, a selective PKC inhibitor, failed to prevent the inhibition by UCN, indicating that PKC is also not involved in $Ca_V3.2$ channel inhibition. Previous reports have suggested that PLC activation could also be part of the CRFR1-signaling pathway (Radulovic et al., 2003). PLC is a critical component of the phosphoinositol pathway that generates two second messengers, diacylglycerol and inositol 1,4,5-trisphosphate, that are thought to be involved in some types of T-type calcium channel regulation (Chemin et al., 2006). We found that U-73122, a phospholipase C inhibitor, was unable to abrogate the inhibition of $Ca_V3.2$ induced by the UCN-mediated activation of CRFR1 receptor, ruling out the possible involvement of the PLC pathway. Furthermore, the inhibition of $Ca_V3.2$ channels via the CRFR1 receptor is independent of the activation of tyrosine kinases, CaMKII, and PI3K, through which T-type calcium channels could be regulated. The explanation for the differences remains to be determined, but it might be attributed to the diversity of UCN activities on cells or that the A-kinase-anchoring protein-deficient HEK293 cells may not be capable of supporting robust ion channel phosphorylation. In addition, it has been reported that kinase modulation of T-type calcium channels has been shown to be temperature-dependent in which phosphorylation was observed at 37°C, but it was less obvious when the experiments were performed at room temperature (Chemin et al., 2007). These factors may be involved in CRFR1-mediated $Ca_V3.2$ regulations, and they need to be further examined.

Native and cloned T-type calcium channel properties have been reported to be regulated by cAMP-dependent PKA, PKC, PKG, calmodulin-dependent protein kinase II, and tyrosine kinases through various G protein-coupled receptors (Herrington and Lingle, 1992; Kim et al., 2006). We find that $G_{\beta 2}$ and $G_{\gamma 2}$ transcripts and proteins are endogenously expressed in HEK293 cells, which suggests the potential involvement of $G_{\beta 2}$ in the selective inhibition of $Ca_V3.2$ channels by activation of the CRFR1 receptor. However, other possible subtypes of G protein $\beta\gamma$ subunits could not be excluded, and they need to be further investigated. Previous reports have shown that activation of dopamine D1 and D2 receptors could mediate the T-type calcium channels inhibition (Wolfe et al., 2003; Chemin et al., 2006). Nevertheless, the inhibitory mechanism of $Ca_V3.2$ channels mediated by CRFR1 receptor is distinctly different from the activation of

the dopamine receptors (Wolfe et al., 2003). Our data suggested that the CRFR1-mediated selective inhibition of $Ca_V3.2$ was through the stabilization of the channels in their inactivated state, whereas activation of D1 receptors reduces the open probability of the $Ca_V3.2$ channels, and the voltage-dependent steady-state inactivation of the channels remains unchanged. Evidence to suggest our conclusion includes 1) robust hyperpolarized shift of voltage-dependent steady-state inactivation, 2) reversal of the hyperpolarized shift of inactivation potentials after introduction of the QEHA competitor peptide or the washout of UCN from the bath solution, and 3) a reduction in the concentration of UCN to trigger inhibition of $Ca_V3.2$ channels when cells are held at the more depolarized membrane potential of −80 mV compared with that for −110 mV. However, a comparison of the rat $Ca_V3.2$ (AF290213) used in this report with the human $Ca_V3.2$ channel used by the Barrett's group (AF290213) did not show obvious differences in the choice of alternatively spliced exons. But, the two clones contained differences in amino acid residues that code for the II-III linker. Whether these species differences in the cytoplasmic regions of the channels, including the II-III linker, are important to account for the differences in mechanisms for inhibition by CRFR1 and dopamine receptors require future work. Besides, we used a 15-s protocol that is different from the 6-s voltage prepulses used by the Barrett's group (Wolfe et al., 2003). This difference in experimental protocol may be relevant as it has been demonstrated that a shorter duration of the prepulse resulted in a depolarizing shift in the steady-state inactivation in the $G\beta\gamma$-mediated inhibition of $Ca_V2.2$ channels (McDavid and Currie, 2006). Nonetheless, besides the observed hyperpolarized shift in steady-state inactivation, we cannot exclude the possibility that the probability of opening of the $Ca_V3.2$ channels may also be reduced upon activation of CRFR1 receptors by UCN. There is a possibility that both mechanisms act as a unified pathway to inhibit the $Ca_V3.2$ currents upon activation of CRFR1 receptors by UCN.

In the present study, we found that G protein-mediated $Ca_V3.2$ channels inhibition was reversible, which is consistent with the previous reports about Ca_V2 channels. However, our result showed that the kinetics of $Ca_V3.2$ channels inhibition induced by CRFR1 activation seemed to be slow, whereas $G\beta\gamma$ inhibition of Ca_V2 channels was very fast (De Waard et al., 1997). The explanation for the differences remains to be determined, but it might be attributed to channel internalization during the slowly developing process or to the diversity of UCN activities on cells. In addition, whereas $G\beta\gamma$ subunits inhibit high-voltage-gated Ca_V2 calcium channels via binding to the I-II linker region, they distinctly bind to the II-III linker of $Ca_V3.2$ channels (Ikeda, 1996; Zamponi and Snutch, 1998). The binding of the $G\beta\gamma$ subunits to $Ca_V2.2$ channels has been reported to alter the voltage-dependent activation or inactivation properties of the channels, depending upon the frequency of the action potential-like waveforms examined (Zamponi and Snutch, 1998). Using low-frequency action potential-like waveforms, $Ca_V2.2$ N-type channels display a depolarizing shift in the steady-state inactivation potentials when the conditioning pulse is applied for 3 s (McDavid and Currie, 2006). Given that the $G\beta\gamma$ effects on $Ca_V2.2$ N-type channels can vary depending upon the nature of the stimulus, future studies will be required to dissect the differences in the effects on steady-state inactivation properties of $Ca_V3.2$ channels observed after activation of CRFR1. Recent studies by Iftinca and colleagues have identified a depolarizing shift on $Ca_V3.2$, but not $Ca_V3.1$ and $Ca_V3.3$, inactivation properties in response to Rho-associated kinase activation via the endogenous ligand lysophosphatidic acid (Iftinca et al., 2007). Like $G\beta\gamma$ regulation on $Ca_V3.2$ channels, this mechanism involved the II-III loop, and it is tempting to speculate the existence of cross talk between these two regulatory pathways.

In conclusion, the present study provides evidence that activation of CRFR1 results in the selective inhibition of $Ca_V3.2$ T-type calcium currents, whereas $Ca_V3.1$ and $Ca_V3.3$ were not affected. The mechanism for the inhibition was via a cholera toxin-sensitive, $G\beta\gamma$-mediated signaling pathway that resulted in a hyperpolarized shift in the steady-state inactivation property of the $Ca_V3.2$ calcium channels. Note that the effect is reversible upon washout of the CRFR1 receptor agonists such as CRF or UCN. As UCN affect multiple aspects of cardiac and neuronal physiology and as $Ca_V3.2$ channels are expressed widely throughout the cardiovascular and nervous systems, our results point to a novel and functionally relevant CRFR1-calcium channel signaling pathway. In future experiments, it will be interesting to determine whether selective inhibition of $Ca_V3.2$ calcium channels via activation of CRFR1 receptors may directly play a role in stress response, affective disorders, or in cardiovascular pathophysiology.

Acknowledgments

We thank Dr. Brett Adams for the kind gifts of MAS-GRK3ct and EGFP-RGS2 and Dr. David Parker for the human $Ca_V3.1$, $Ca_V3.2$, and $Ca_V3.3$ T-type calcium channels. We also thank Tan Fong Yong and Dejie Yu for excellent technical assistance.

References

Bale TL and Vale WW (2004) CRF and CRF receptors: role in stress responsivity and other behaviors. *Annu Rev Pharmacol Toxicol* **44:**525–527.

Bourinet E, Alloui A, Monteil A, Barrere C, Couette B, Poirot O, Pages A, McRory J, Snutch TP, Eschalier A, et al. (2005) Silencing of the $Ca_V3.2$ T-type calcium channel gene in sensory neurons demonstrates its major role in nociception. *EMBO J* **24:**315–324.

Bruijnzeel AW and Gold MS (2005) The role of corticotrophin-releasing factor peptides in cannabis, nicotine, and alcohol dependence. *Brain Res Rev* **49:**505–528.

Chalmers DT, Lovenberg TW, and De Souza EB (1995) Localization of novel corticotropin-releasing factor receptor (CRF2) mRNA expression to specific subcortical nuclei in rat brain: comparison with CRF1 receptor mRNA expression. *J Neurosci* **15:**6340–6350.

Chemin J, Traboulsie A, and Lory P (2006) Molecular pathways underlying the modulation of T-type calcium channels by neurotransmitters and hormones. *Cell Calcium* **40:**121–134.

Chemin J, Mezghrani A, Bidaud I, Dupasquier S, Marger F, Barrère C, Nargeot J, and Lory P (2007) Temperature-dependent modulation of Ca_V3 T-type calcium channels by protein kinases C and A in mammalian cells. *J Biol Chem* **282:**32710–32718.

Cribbs LL, Lee JH, Yang J, Satin J, Zhang Y, Daud A, Barclay J, Williamson MP, Fox M, Rees M, et al. (1998) Cloning and characterization of alpha1H from human heart, a member of the T-type Ca^{2+} channel gene family. *Circ Res* **83:**103–109.

Dautzenberg FM, Higelin J, and Teichert U (2000) Functional characterization of corticotropin-releasing factor type 1 receptor endogenously expressed in human embryonic kidney 293 cells. *Eur J Pharmacol* **390:**51–59.

Dautzenberg FM and Hauger RL (2002) The CRF peptide family and their receptors: yet more partners discovered. *Trends Pharmacol Sci* **23:**71–77.

De Waard M, Liu H, Walker D, Scott VE, Gurnett CA, and Campbell KP (1997) Direct binding of G-protein betagamma complex to voltage-dependent calcium channels. *Nature* **385:**446–450.

Drolet P, Bilodeau L, Chorvatova A, Laflamme L, Gallo-Payet N, and Payet MD (1997) Inhibition of the T-type Ca^{2+} current by the dopamine D1 receptor in rat adrenal glomerulosa cells: requirement of the combined action of the G betagamma protein subunit and cyclic adenosine 3′,5′-monophosphate. *Mol Endocrinol* **11:**503–514.

Gravanis A and Margioris AN (2005) The corticotrophin-releasing factor (CRF) family of neuropeptides in inflammation: potential therapeutic applications. *Curr Med Chem* **12:**1503–1512.

Herrington J and Lingle CJ (1992) Kinetic and pharmacological properties of low voltage-activated Ca^{2+} current in rat clonal (GH3) pituitary cells. *J Neurophysiol* **68:**213–232.

Hildebrand ME and Snutch TP (2006) Contributions of T-type calcium channels to the pathophysiology of pain signaling. *Drug Discov Today Dis Mech* **3:**335–341.
Hockberger P, Toselli M, Swandulla D, and Lux HD (1989) A diacylglycerol analogue reduces neuronal calcium currents independently of protein kinase C activation. *Nature* **338:**340–342.
Iftinca M, Hamid J, Chen L, Varela D, Tadayonnejad R, Altier C, Turner RW, and Zamponi GW (2007) Regulation of T-type calcium channels by Rho-associated kinase. *Nat Neurosci* **10:**854–860.
Ikeda SR (1996) Voltage-dependent modulation of N-type calcium channels by G-protein $\beta\gamma$ subunits. *Nature* **380:**255–258.
Jagannathan S, Punt EL, Gu Y, Arnoult C, Sakkas D, Barratt CL, and Publicover SJ (2002) Identification and localization of T-type voltage-operated calcium channel subunits in human male germ cells. *J Biol Chem* **277:**8449–8456.
Kammermeier PJ and Ikeda SR (1999) Expression of RGS2 alters the coupling of metabotropic glutamate receptor 1a to M-type K^+ and N-type Ca^{2+} channels. *Neuron* **22:**819–829.
Kim JA, Park JY, Kang HW, Huh SU, Jeong SW, and Lee JH (2006) Augmentation of $Ca_V3.2$ T-type calcium channel activity by cAMP-dependent protein kinase A. *J Pharmacol Exp Ther* **318:**230–237.
Kim Y, Park MK, Uhm DY, and Chung S (2007) Modulation of T-type Ca^{2+} channels by corticotropin-releasing factor through protein kinase C pathway in MN9D dopaminergic cells. *Biochem Biophys Res Commun* **358:**796–801.
Lee AK and Tse A (1997) Mechanism underlying corticotropin-releasing hormone (CRH) triggered cytosolic Ca^{2+} rise in identified rat corticotrophs. *J Physiol* **504:**367–378.
Markovic D, Papadopoulou N, Teli T, Randeva H, Levine MA, Hillhouse EW, and Grammatopoulos DK (2006) Differential responses of corticotropin-releasing hormone receptor type 1 variants to protein kinase C phosphorylation. *J Pharmacol Exp Ther* **319:**1032–1042.
McDavid S and Currie KP (2006) G-proteins modulate cumulative inactivation of N-type ($Ca_V2.2$) calcium channels. *J Neurosci* **26:**13373–13383.
McKay BE, McRory JE, Molineux ML, Hamid J, Snutch TP, Zamponi GW, and Turner RW (2006) Ca_V3 T-type calcium channel isoforms differentially distribute to somatic and dendritic compartments in rat central neurons. *Eur J Neurosci* **24:**2581–2594.
McRory JE, Santi CM, Hamming KS, Mezeyova J, Sutton KG, Baillie DL, Stea A, and Snutch TP (2001) Molecular and functional characterization of a family of rat brain T-type calcium channels. *J Biol Chem* **276:**3999–4011.
Molineux ML, McRory JE, McKay BE, Hamid J, Mehaffey WH, Rehak R, Snutch TP, Zamponi GW, and Turner RW (2006) Specific T-type calcium channel isoforms are associated with distinct burst phenotypes in deep cerebellar nuclear neurons. *Proc Natl Acad Sci U S A* **103:**5555–5560.
Nelson MT, Todorovic SM, and Perez-Reyes E (2006) The role of T-type calcium channels in epilepsy and pain. *Curr Pharm Des* **12:**2189–2197.
Nuss HB and Houser SR (1993) T-type Ca^{2+} current is expressed in hypertrophied adult feline left ventricular myocytes. *Circ Res* **73:**777–782.
Perez-Reyes E (2003) Molecular physiology of low-voltage-activated T-type calcium channels. *Physiol Rev* **83:**117–161.
Radulovic M, Hippel C, and Spiess J (2003) Corticotropin-releasing factor (CRF) rapidly suppresses apoptosis by acting upstream of the activation of caspases. *J Neurochem* **84:**1074–1085.
Reul JM and Holsboer F (2002) Corticotropin-releasing factor receptors 1 and 2 in anxiety and depression. *Curr Opin Pharmacol* **2:**23–33.
Steriade M and Llinas RR (1988) The functional states of the thalamus and the associated neuronal interplay. *Physiol Rev* **68:**649–742.
Suh BC and Hille B (2002) Recovery from muscarinic modulation of M current channels requires phosphatidylinositol 4,5-bisphosphate synthesis. *Neuron* **35:**507–520.
Talley EM, Cribbs LL, Lee JH, Daud A, Perez-Reyes E, and Bayliss DA (1999) Differential distribution of three members of a gene family encoding low voltage-activated (T-type) calcium channels. *J Neurosci* **19:**1895–1911.
Tao J, Wu Y, Chen J, Zhu H, and Li S (2005) Effects of urocortin on T-type calcium currents in mouse spermatogenic cells. *Biochem Biophys Res Commun* **329:**743–748.
Welsby PJ, Wang H, Wolfe JT, Colbran RJ, Johnson ML, and Barrett PQ (2003) A mechanism for the direct regulation of T-type calcium channels by Ca^{2+}/calmodulin-dependent kinase II. *J Neurosci* **23:**10116–10121.
Wolfe JT, Wang H, Howard J, Garrison JC, and Barrett PQ (2003) T-type calcium channel regulation by specific G-protein $\beta\gamma$ subunits. *Nature* **424:**209–213.
Zamponi GW and Snutch TP (1998) Modulation of voltage-dependent calcium channels by G-proteins. *Curr Opin Neurobiol* **8:**351–356.

Address correspondence to: Dr. Tuck Wah Soong, Department of Physiology, Yong Loo Lin School of Medicine, National University of Singapore, Singapore 117597. E-mail: phsstw@nus.edu.sg